Journal of Earth Science, *Vol. 23*, *No. 4*, *p. 421–430*, *August 2012* *ISSN 1674-487X*
Printed in China
DOI: 10.1007/s12583-012-0265-2

Seismic Reflection, Distribution, and Potential Trap of Permian Volcanic Rocks in the Tahe Field

Renhai Pu* (蒲仁海), **Yunlong Zhang** (张云龙), **Jinglan Luo** (罗静兰)
State Key Laboratory of Continental Dynamics, *Northwest University*, *Xi'an* 710069, China;
Department of Geology, *Northwest University*, *Xi'an* 710069, China

ABSTRACT: Permian Kaipaileicike (开派雷兹克) volcanic rocks approximately 0–200 m thick are drilled in the Tahe (塔河) field. The distribution of volcanic rocks and their potential to form hydrocarbon reservoirs are discussed based on the integrated interpretation of log and 3D seismic data. The volcanic rocks, mainly consisting of dacites and basalts, are sandwiched between the Lower Triassic and Lower Carboniferous and bounded by top and bottom unconformities. The dacites accumulated in a mound shape around volcanic craters, whereas the basalts are deposited in tabular or trough-fill geometries. Permian volcanic craters mainly located at the northwest corner of the Tahe field are identified from volcanic rock thickening, occurrence of volcanic breccias, structural arch of the top Permian, seismic attribute anomalies, and fault (piercing conduit) reflections. Along the northwest wing of a Carboniferous salt dome, a stratigraphic trap is formed by a northeast updip pinch-out of Permian volcanic rock. Oil indications within the trap are found in numerous wells. The reservoir volcanic rocks are mainly of the fracture-pore pattern and covered by the caprock of a Lower Triassic mudstone. The hydrocarbon reservoir, which can potentially be a medium-sized oil pool, is connected to Cambrian–Ordovician source rocks through normal faults along the salt dome boundary.

KEY WORDS: volcanic crater, volcanic seismic facies, volcanism distribution, volcanic reservoir.

INTRODUCTION

In the past years, a large number of oil and gas pools related to volcanic rocks have been found in the Songliao basin, Junggar basin, and Santanghu basin in China (Liu et al., 2009; Jin et al., 2008; Zhao et al., 2008; Taner et al., 1988). The volcanic rock reservoir is an important type of oil and gas pool. Two sets of basic and acidic Permian volcanism cycles developed in Tarim basin, corresponding to the Kupukuciman Formation and the Kaipaileicike Formation, respectively (Pu et al., 2011; Sun et al., 1993). Only the Kaipaileicike Formation in the Tahe oilfield of the northern Tarim basin is drilled by production wells of the Ordovician pools (Liu et al., 2011). Some Permian volcanic rocks in these wells indicate oil (Luo et al., 2006; Yang et al., 2004). However, their ability to form commercial oil reservoirs still needs to be determined by geologists. The current study aims to characterize the seismic reflection of different volcanic rocks and craters based on well and 3D seismic data. Moreover, the subsequent pinch-out line and top structure of volcanic rocks are analyzed to evaluate potential traps and pools.

This study was supported by the SINOPEC Forward Looking Project (No. YPH08114) and the National Key Project of China (No. 2011zx05001-003).

*Corresponding author: purenhai@nwu.edu.cn

Manuscript received January 20, 2012.
Manuscript accepted April 12, 2012.

In the Tahe oilfield, tens of wells reveal Permian volcanic rocks 0–200 m thick and are mainly composed of basalt and dacite rocks, with a small amount of interbedded random volcanic breccias and tuff. The Permian volcanic rocks are bounded by top and bottom unconformities and sandwiched between the lacustrine mudstone of the Lower Triassic Ketuer Formation and the terrestrial sandstone and mudstone of the Lower Carboniferous Kalashayi Formation. Based on a synthetic seismogram and horizon calibration, the top Permian volcanic rock is calibrated at a wave peak and is referred to as the T_5^0 reflection on seismic profiles, and the bottom volcanic rock is calibrated at different positions with the change in Permian thickness (Fig. 1).

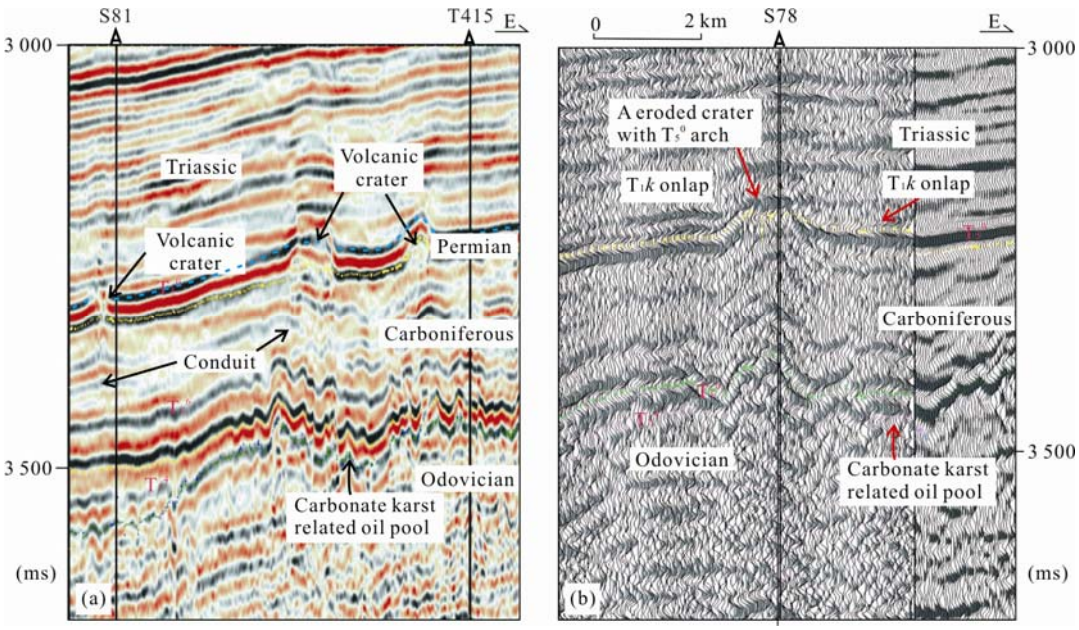

Figure 1. 3D seismic sections showing volcanic craters. (a) The S81 and T415 well-linked section with three volcanic craters indicated by the arch as well as interruptions of the top Permian T_5^0 high amplitude reflection. (b) The arch of the volcanic conduit and crater and the absence of Permian volcanic rocks as a result of erosion at the crater drilled by Well S78.

IDENTIFICATION OF VOLCANIC CRATERS AND CONDUITS

Volcanic craters in the Tahe field have the following identifying features based on the 3D seismic profiles.

Arch Reflection of Top Volcanic Rocks (T_5^0)

Similar to modern craters seen on the ground surface, the ancient crater also formed a positive landscape on the top surface of volcanic rocks. The positive landscape appears as an arch reflection of the top volcanic rocks. Arch reflections are absent in both the Permian interior and the overlying Triassic, indicating that the arch is not related to a structural anticline but to the lava eruption at the volcanic conduit (Fig. 1a). The higher parts of the ancient crater eroded sometime before the Triassic deposition, which may have resulted in the loss of volcanic rocks, and the top surface of the crater was stripped into a platform, such as the S78 well drilled rightly on the crater (Fig. 1b). The lower parts of the top Permian hardly suffer from post-volcanic erosion, and the most craters can be preserved as mound-shaped reflections, such as those seen at wells S55 and S99 (Fig. 2).

Low Amplitude and Coherence Value Anomalies

Being at a higher structure, the volcanic rocks near the craters were eroded, which led to the decrease in the amplitude of the T_5^0 reflection of the craters (Fig. 1). Magma eruption and fault activity at the

conduits broke or displaced the T_5^0 event to form the low coherence value anomaly of the craters on the coherence map at a window 15 ms downard from T_5^0 (Brown, 1999, see part 4).

Volcanic Rock Thickening around the Craters

Volcanism in the Tahe field is susceptible to faults. In general, volcanic rocks tend to increase in thickness along faults or at the intersection of two sets of faults. In particular, acid volcanic rocks accumulate and thicken as mound reflections around the craters (Fig. 4).

Accumulation of Volcanic Explosive Facies near the Craters

The rock types of volcanic explosive facies include breccias lava, tufflava, lava tuff, and volcanic breccia. The closer the planar position to the craters, the coarser the breccias. According to the core statistics and comprehensive log data, the explosive indices (percentage of breccia thickness to the total thickness of the volcanic rocks) of wells S98, T208, S10, S91, S76, and S99 in the Tahe field are 34.8, 24.3, 21.5, 18.3, 10.5, and 8.9, respectively. These wells, which are associated with the types and distribution of the volcanic rocks, are presumed located at a possible volcanic explosive eruption facies; the volcanic eruptive center is located at the facies as well (Luo et al., 2006).

BASALT AND DACITE REFLECTIONS

Based on the well-linked 3D seismic profiles, two of the most important volcanic rocks in the Tahe field, dacite and basalt, exhibit significantly different features (Fan and Pu, 2005). Whenever the basalt appears alone, as seen in Well S10, or coexists with the overlying dacite (as seen in wells S86, S91, T705, S87, and T207), the basalt has always been of the trough-fill reflection geometry (Figs. 2–4). Moreover, the reflection amplitude in its interior is always

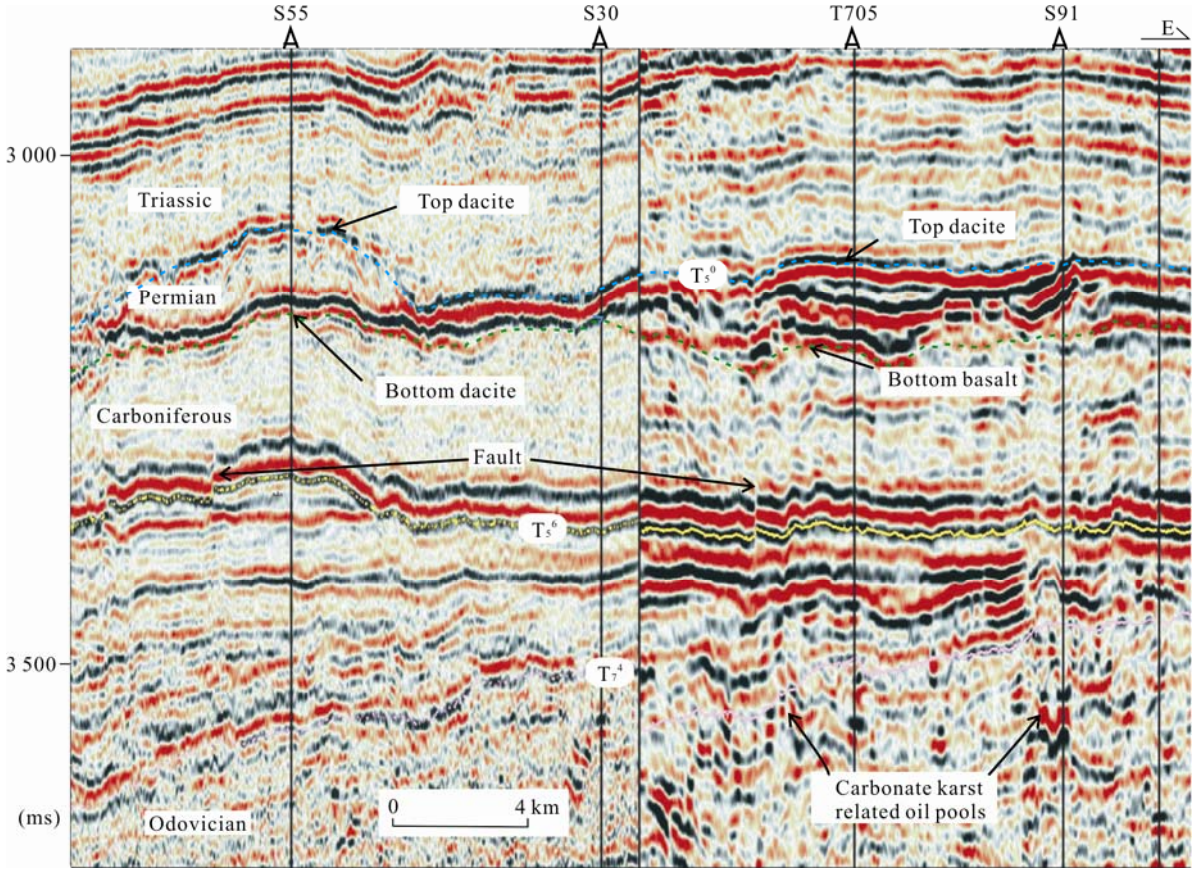

Figure 2. 3D seismic section of wells S55, S30, T705, S91, and T707 showing the Permian mound-shaped dacite and the trough-fill-shaped basalt.

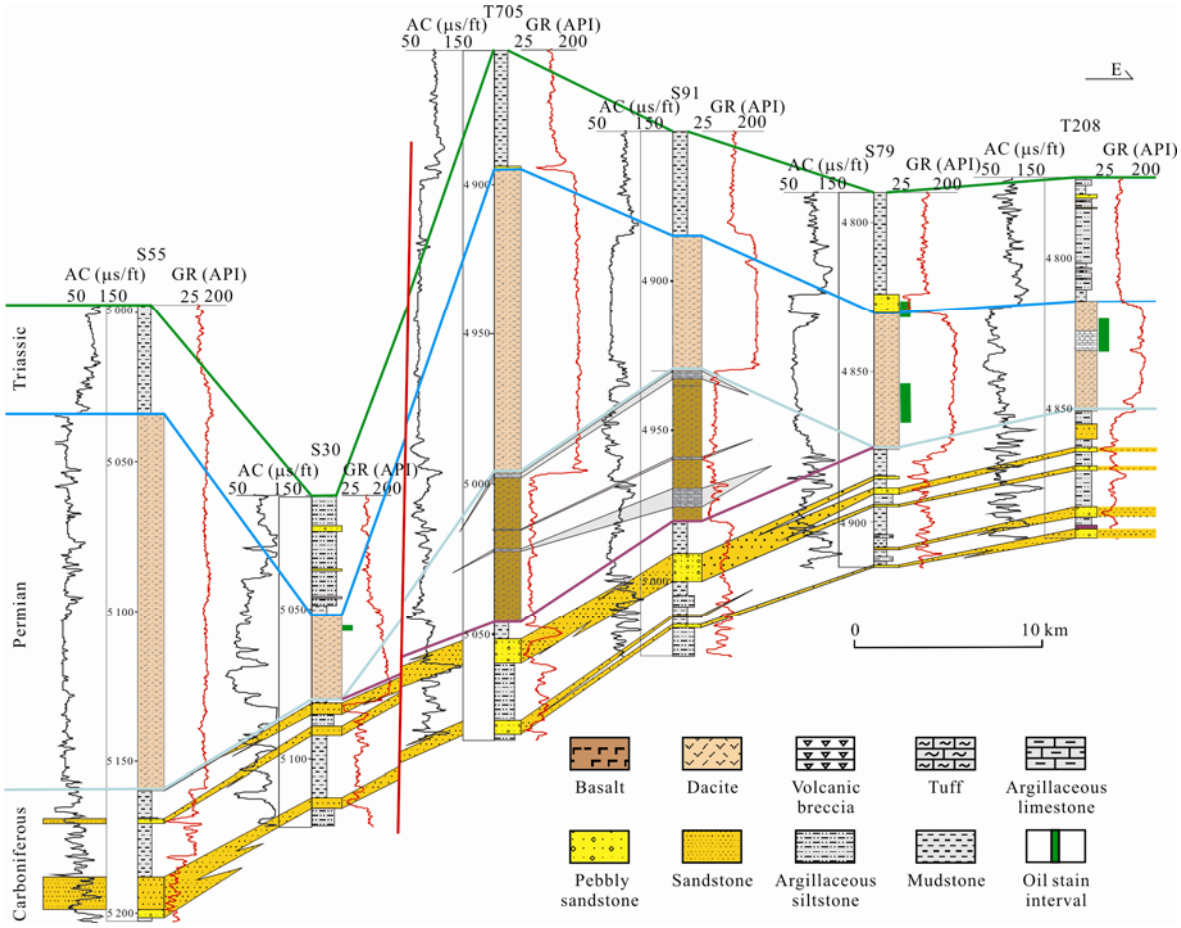

Figure 3. Cross-section of the Permian volcanic rock of wells S55, S30, T705, S91, S78, and T208.

strong. When only dacite is distributed (without basalt), a weak amplitude of hummocky reflection is formed as seen in Well S55 (Figs. 2 and 3).

The trough-fill reflection of basalt indicates low viscosity and easy-flowing basic magma, whose distribution is obviously susceptible to paleotopography. According to an earlier research, magma viscosity depends on the mineral composition and temperature. The viscosity is generally large when the SiO_2 and Al_2O_3 contents are high and FeO and MgO are low and vice versa (Xu and Qiu, 1985). Thus, the viscosity of basaltic magma is lower than that of dacite, and the former more easily flows than the latter. Acidic magma, which has a temperature of nearly 750–800 ℃), has a high viscosity and would rapidly curdle when erupted to the ground surface. On the other hand, basic magma is generally 900–1 300 ℃) in temperature and can generally flow when erupted to the ground surface at a very low velocity (generally <16 km/h). The flow velocity can sometimes reach as high as 30 km/h. The strong reflections within the basalt interior may be the result of low impedance of the interbedded tuff and volcanic breccia or the remarkable impedance difference from the overlying dacite. Sonic log data show that the velocity of basalt (5 000–6 000 m/s) is slightly higher than that of dacite (4 700–5 500 m/s), which in turn is higher than that of tuff (3 800–4 700 m/s).

Hummocky dacite results from a high viscosity and rapid accumulation of acidic magma around craters. The weak amplitude within the thick dacite suggests a uniform lithology, without the presence of other interbedded rocks. A dacite mound is likely to form hydrocarbon traps. The upper volcanic rocks usually contain gas vugs and fractures formed during diagenesis and are possibly weathered and dissolved by epigenetic leaching relative to the top bounded unconformity. On the other hand, the mound is also

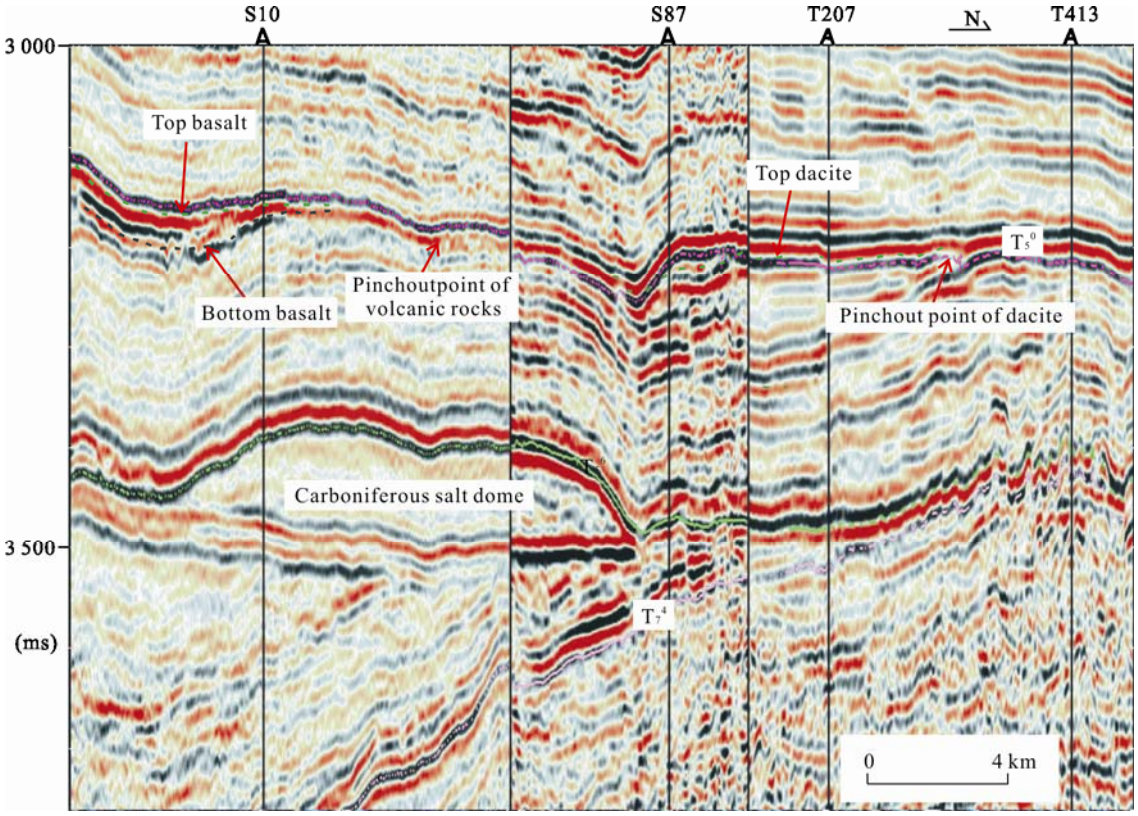

Figure 4. A well-linked seismic section showing the reflection geometry of basalt and dacite. Only basalt is present in Well S10 and its reflection is of the trough-fill shape. Only the dacite is encountered in wells S87 and S207 and its reflection is of mound to tabular shapes.

conducive to trap formation because of its positive structure.

UNCONFORMITY REFLECTIONS OF THE TOP AND BOTTOM VOLCANIC ROCKS

Based on 3D seismic sections, unconformity reflections exist on both the top and bottom Permian volcanic rocks. Truncation and onlap unconformities of the top volcanic rocks are distinct and common. The Permian craters are truncated or even completely eroded (Fig. 1). Triassic can sometimes be seen to onlap toward the top volcanic rocks of high structure or onlap at the flanks of the hummocky dacite (Fig. 2). Carboniferous Kalashayi Formation is randomly truncated by the bottom volcanic reflection, as seen in the S10–S702 well-linked SN seismic sections (Fig. 5), although most of the bottom volcanic rocks are parallel to the underlying strata. The hiatus indicated by the unconformities at the top and bottom volcanic rocks is consistent with the paleontological and isotopic dating of volcanic rocks (Yu et al., 2011; Luo et al., 2006).

VOLCANIC ROCK PINCH-OUT AND THICKNESS VARIATIONS

Volcanic rocks are thinned and pinch-out on seismic sections via two ways. One is the rapid pinching out of thick volcanic rocks at a short distance. The other involves the slow pinching out of thin volcanic rocks at a large distance. The former is often represented by a reflection termination and thus can be easily recognized (Figs. 4 and 5). The latter does not cause an event termination and needs to be identified by the decrease in the T_5^0 amplitude. Therefore, identifying the pinch-out line of volcanic rocks using 3D seismic data is somewhat difficult and uncertain. When the thickness of the volcanic rocks is approximately 46 m, the T_5^0 tuning amplitude reaches the maximum as a result of the constructive interference of the top and bottom reflections of the volcanic rocks. The T_5^0 amplitude gradually decreases with decreasing volcanic rock thickness. However,

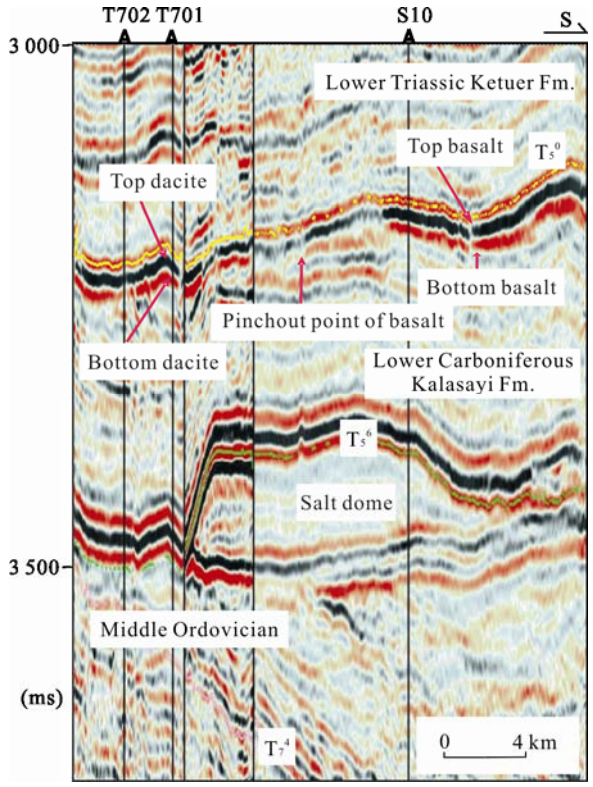

Figure 5. Truncation unconformity of the bottom Permian and pinch-out refliction of volcanic rocks.

when the volcanic rocks thin to 0 m, the T_5^0 reflection remains and maintains a definite amplitude because of the remarkable difference between the impedances of the overlying Ketuer Formation and the underlying Kalashayi Formation. On the T_5^0 amplitude map, the pinch-out line of the volcanic rocks can roughly be delineated as the boundary line between the strong and weak amplitudes (blue and green regions in Fig. 6, respectively). Moreover, the amplitude is weak when the volcanic thickness is greater than the tuning thickness (46 m). For example, as shown in Fig. 6, the volcanic rocks of wells T453, T701, and S87 are 87, 139, and 89 m, respectively, which are all greater than the tuning thickness; thus, the amplitudes at these wells are all weak.

The top and bottom interfaces of the volcanic rocks are traced on 3D seismic profiles based on horizon calibration of 32 wells drilling into volcanic rocks. The isopach map of the volcanic rocks is obtained using the half difference between the bottom and top horizons isochron map, multiplied by the velocity map of the volcanic rocks. The volcanic rocks revealed by the boreholes are 7–514.5 m thick (average, 110.1 m). The volcanic rocks overall become thiner and pinch-out updip northeastward (Fig. 7). Although some craters exist on the northern part of the Tahe field, volcanic rocks are absent in the area because of subsequent denudation. The volcanic rocks are spread out within a NEE belt approximately 8 km wide and more than 20 km long and drilled by wells S76, T701, S87, S79, and T208.

The planar change in thickness of the volcanic rocks is relevant to volcanic lithology, the distance to the volcanic crater, and the ancient structure or topography. In the study area, there are three thickening belts and one thinning belt (Fig. 7), as follows.

(1) Basalt thickening belt at the southwest Well S10: basalt thickens toward this area as a result of a lower ancient structure or topography.

(2) NEE thickening belt along a salt edge: volcanic rock thickness increases within a salt-edge depression because of the deformation of a Carboniferous salt dome.

(3) Dacite hummocky thickening belt near wells S55–S99: dacite of high viscosity (i.e., slow-flowing) accumulates around the crater.

(4) Thinning and absence belt at Well X1: A Permian hiatus exists on the ancient high structure where no volcanic rocks are deposited; Carboniferous–Triassic layer become thin on this belt.

POTENTIAL VOLCANIC ROCK TRAP

Most volcanic rock reservoirs consist of dacite, whereas others consist of basalt and tuff. A fracture-pore assemblage is the main pore type. Fractures are relatively well developed and become important factors in improving the reservoir quality. Volcanic explosive facies are favorable reservoir belts. Effusive facies lava located at the ancient eroded slope and higher structures forms more valuable reservoirs, which are drilled by wells S10, S30, S55, S79, S87, T208, and others. The top and upper parts of the lava contain both higher primary gas pores and secondary dissolved vugs, which can serve as beneficial reservoir intervals. Based on 45 core samples of volcanic rocks in the Tahe field, the measured volcanic rock porosity ranges from 0.1% to 19.4%, with an average of 5.7%. Moreover, the

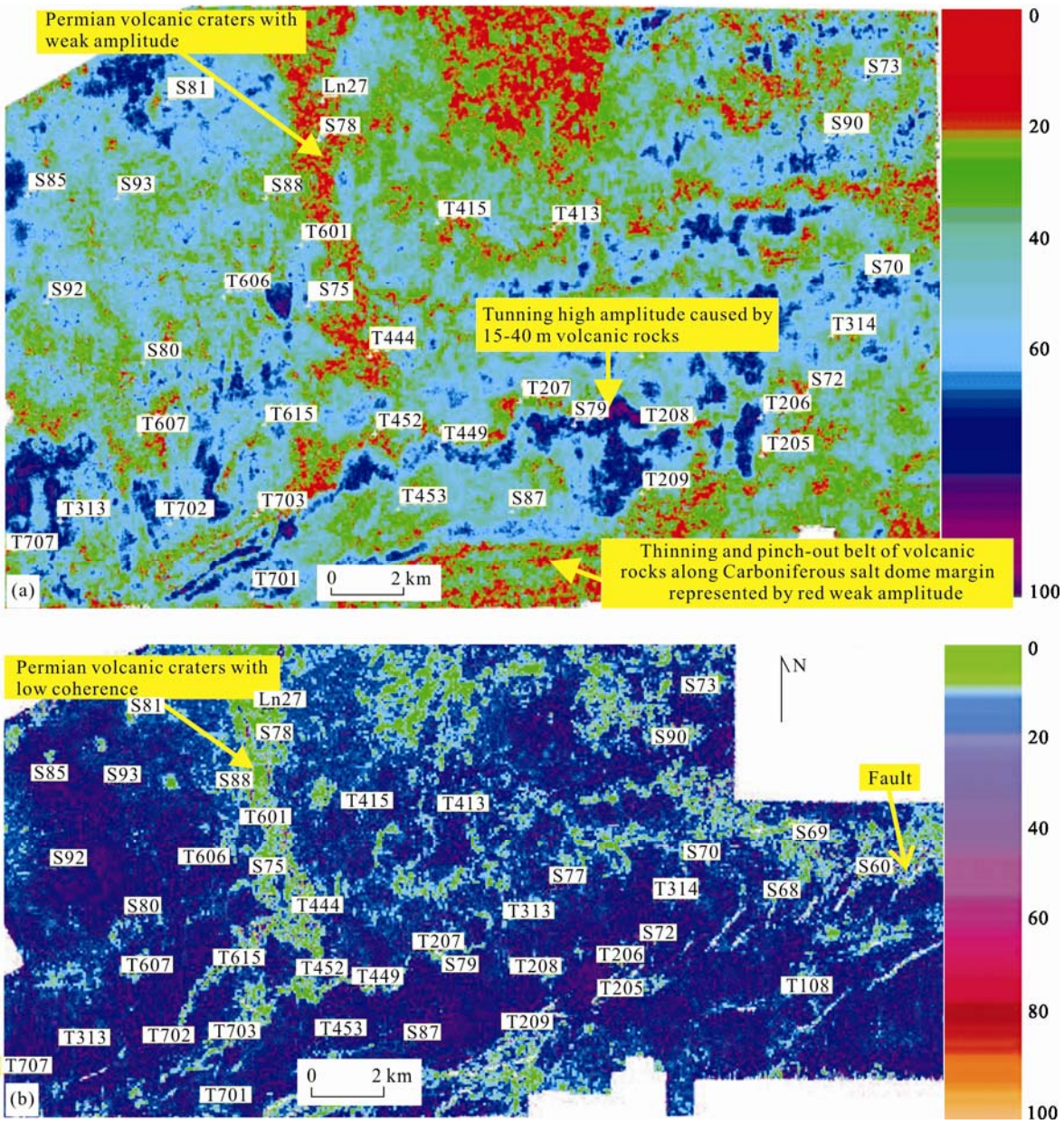

Figure 6. 3D average amplitude map (a) and coherence map (b) of a 15 ms window downward from the top Permian T_5^0 at the mid-east of the Tahe field. Volcanic crater distribution and pinch-out line of volcanic rocks can be scrutinized from the variation in amplitude and coherence atrributes.

measured permeability ranges from 0.01×10^{-3} to 10.46×10^{-3} μm^2, with an average of 1.044×10^{-3} μm^2. The high-porosity planar distribution is consistent with the high permeability and located at the southern area close to Well S98 and the northern area close to wells T615, T443, S79, and T208 (Yang et al., 2004).

Based on the core examination, the volcanic rocks of S30, S87, S79, and T208 are commonly oil-stained, and random rocks contain oil in their fractures (Fig. 3). The oil-water contact is approximately 4 825 m deep based on the oil-stained intervals of Well S79 as well as on the depth map of the top Permian volcanic rocks (Fig. 8). The depth map datum is 900 m above sea level. Wells S79–T208, which has remarkable oil indicators, is located at the higher position of the northeast updip pinch-out trap of the volcanic rocks. Oil accumulation is jointly controlled by the updip trap and a nose structure of the top volcanic rocks (Fig. 8). The trap, which has an area of 40 km^2 and a closure of 55 m, may form a mid-sized

pool. The highest point is buried 4 760 m deep and located at approximately 700 m south of the midpoint between wells T208 and T206, which is 2.2 km away from wells T208 and T206. The volcanic rock reservoir is covered by a 40 m cap rock of the Lower Triassic Ketuer mudstone and is underlain by 570 m of the Lower Carboniferous Kalashayi mudstone and sandstones. Therefore, the updip pinch-out trap of volcanic rocks is sealed from three directions (upper, lower, and flank). NE-oriented normal faults occurring at the southeast flank of the trap may be passages connecting Cambrian–Ordovician hydrocarbon source rocks with the volcanic rock reservoir (Zhai and Yun, 2008).

The reservoir isopach map and the porosity contour map of the volcanic reservoir are constructed based interpretation of log and 3D seismic impedance inversion (Pan et al., 2008; Fig. 9). The reservoirs thickness is between 0 and 80 m, with an average of 30 m. The maximum porosity near Well T208 is 11%, and the minimum is 5%, with an average of approximately 7%. Assuming that the reservoir has an

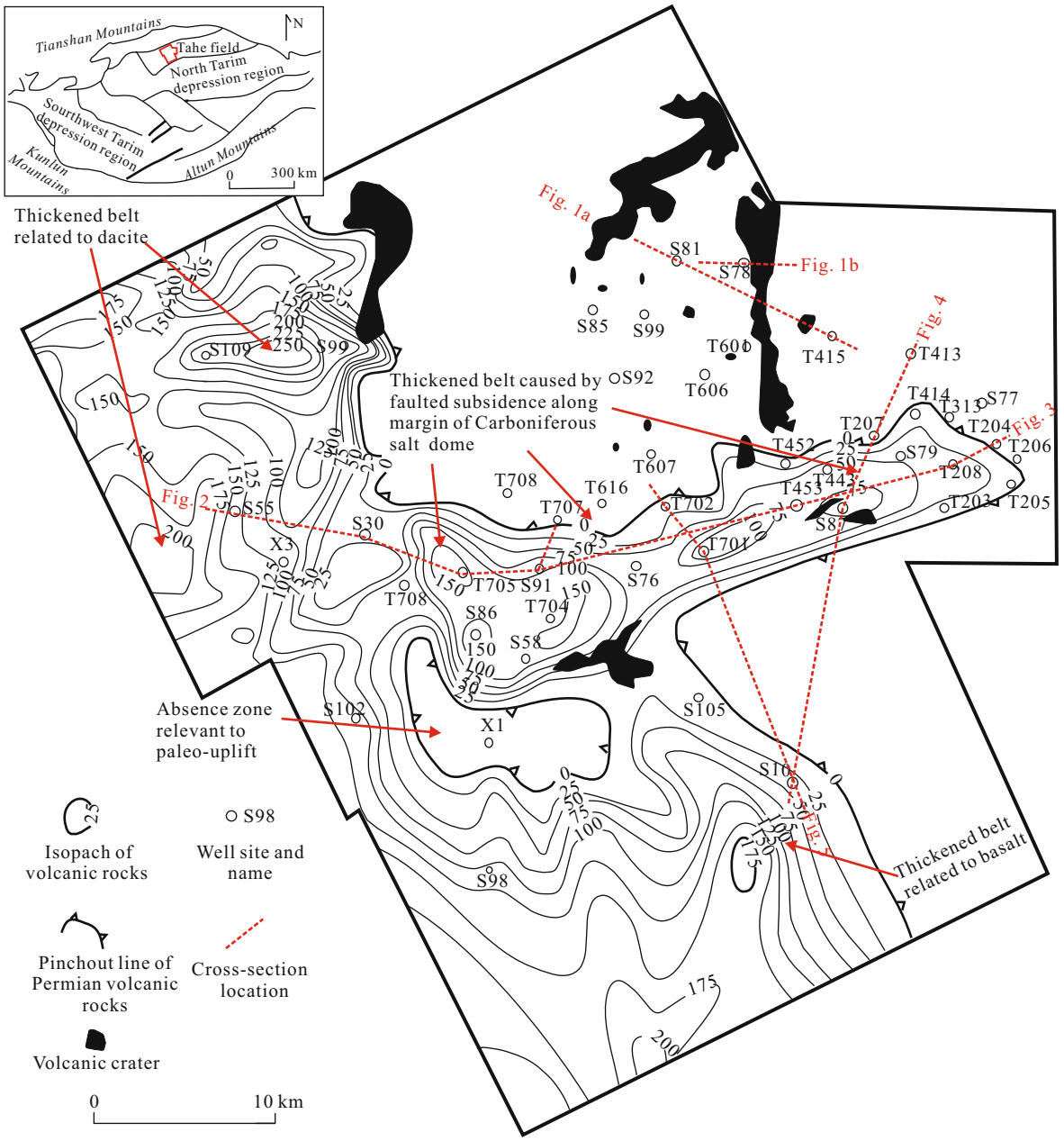

Figure 7. Distribution of the volcanic crater, fault, and isopach map of the volcanic rocks. The location of Tahe field is insetted at the upper left corner.

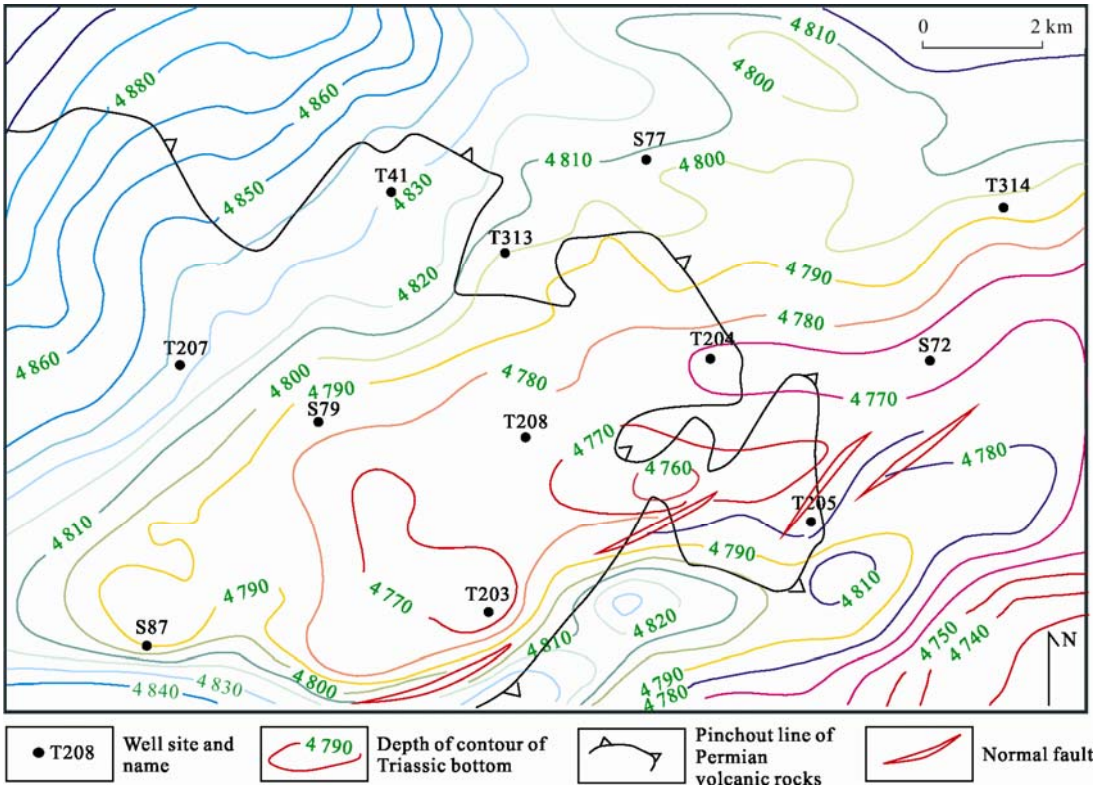

Figure 8. Structural depth contour map of the top of the Permian (900 m a.s.l.).

average thickness of 30 m, an area of 40 km^2, an average effective porosity of 6%, and an average oil saturation of 40%, the volcanic composite trap near Well S79 is estimated to have a gathering capacity of 2 800×10^4 m^3 of crude oil.

CONCLUSIONS

Volcanic craters are mainly distributed at the mid-west part of the Tahe oilfield. They appear as a belt 500–1 000 m wide and 1 000–5 000 m long or as an irregular circle 100–1 000 m in diameter. Craters can be identified based on the following four points: (1) the T_5^0 reflection sharply arches at the craters, but the overlying and underlying reflections are still flat when the Permian is thinned or completely eroded; (2) vertical faults often exist at the volcanic craters; (3) reflections of a high structure or topography, especially for dacite, occur immediately around craters, with an overlapping Triassic layer; and (4) the low coherence and amplitude anomalies of craters appear on 3D seismic attribute maps extracted from the Permian time window.

All top and bottom Permian volcanic rocks are bounded by unconformities. The Tahe field consists of three thickening belts and one thinning belt of volcanic rocks. The first of the three thickening belts is related to the basalt filling into low paleotopography, forming trough-shaped reflections. The second belt is related to the dacite that immediately accumulated around volcanic craters as a hummocky reflection. The last one thickens toward a salt-edge depression caused by the movement of a Carboniferous salt dome and its boundary faults. Two pinch-out patterns of volcanic rocks appear on the 3D seismic data. The first is a rapid pinch-out of thick volcanic rocks at a short distance and is indicated by a seismic event termination. The other is a slow pinch-out of thin volcanic rocks at a long distance, which can be identified based on the decrease in the amplitude of the T_5^0 reflection.

The Permian volcanic rock reservoir is mainly of the fracture-pore pattern and covered by the caprock of a Lower Triassic mudstone. The northeastward updip pinch-out of volcanic rocks in the Tahe field formed a stratigraphic trap on a structural nose background. Hydrocarbon source rocks of a Cambrian–Ordovician origin are connected to the Permian volcanic rock reservoir through normal faults along the salt dome boundary. Oil contained in core fractrues of wells

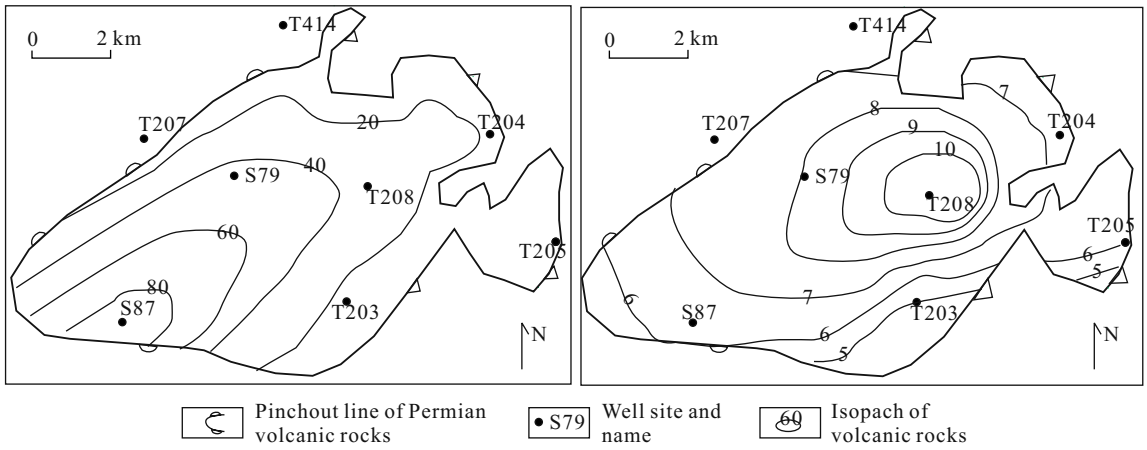

Figure 9. Isopach map of the effective reservoir (left) and porosity contour map of the volcanic reservoir (right) in the traps of Well S79.

drilled at the high trap positions proved the occurrence of oil pool.

REFERENCES CITED

Brown, A. R., 1999. 3D Seismic Interpretation (5th Ed.). *AAPG Mem.*, 40: 187–203

Fan, C. H., Pu, R. H., 2005. Tahe Seismic Reflection Feature and Distribution of Volcanic Rocks. *Science Journal of Northwest University on Line*, 3(4): 0145 (in Chinese with English Abstract)

Jin, J., Liu, L. F., Yu, X. Y., et al., 2008. Progress of Gas Exploration in Carboniferous Volcano Rock in Ludong-Wucaiwan Area, the Junggar Basin. *Natural Gas Industry*, 28(5): 21–23 (in Chinese with English Abstract)

Liu, J. T., Li, H. M., Tan, X. P., et al., 2009. Application of Inversion Technique in Prediction of C_2k Volcanic Rock in Niudong Block. *Progress in Exploration Geophysics*, 32(5): 370–375 (in Chinese with English Abstract)

Liu, X., Guan, P., Pan, W. Q., et al., 2011. Meticulous Characterization of Permian Volcanic Rocks' Spatial Distribution and Its Geological Significance in the Tarim Basin. *Acta Scientianrum Naturalium Universitatis Pekinensis*, 47(2): 315–320 (in Chinese with English Abstract)

Luo, J. L., Zhai, X. X., Pu, R. H., 2006. Horizon, Petrology and Listhofacies of the Volcanic Rocks in the Tahe Oilfield, Northern Tarim Basin. *Chinese Journal of Geology*, 41(3): 378–391 (in Chinese with English Abstract)

Pan, Y., Jiang, Z. G., Pan, M., et al., 2008. Lithology Method for Identification Igneous Logging in West of Northern Tarim Basin. *Journal of Oil and Gas Technology*, 30(1): 260–262 (in Chinese with English Abstract)

Pu, R. H., Dang, X. H., Xu, J., et al., 2011. Permian Division and Correlation and Distribution of Volcanic Rocks of Tarim Basin. *Acta Petrologica Sinica*, 27(1): 166–180 (in Chinese with English Abstract)

Xu, X. S., Qiu, J. X., 1985. Igneous Petrology. Geological Publishing House, Beijing. 66–71 (in Chinese)

Sun, B. N., Shen, G. L., Liu, Y. X., 1993. The Lower Permian of Terrestrian Facies in the Northern Tarim Basion, Southern Xinjiang, China. *Journal of Lanzhou University*, 29(1): 110–115 (in Chinese with English Abstract)

Taner, I., Kamen-Kaye, M., Meyerhoff, A. A., 1988. Petroleum in the Junggar Basin, Northwestern China. *Journal of Southeast Asian Earth Sciences*, 2(3–4): 163–174

Yang, J. L., Luo, J. L., He, F. Q., et al., 2004. Permian Volcanic Reservoir in Tahe Region. *Petroleum Exploration and Development*, 31(4): 44–47 (in Chinese with English Abstract)

Yu, J. C., Mo, X. X., Dong, G. C., et al., 2011. Felsic Volcanic Rocks from Northern Tarim, NW China: Zircon U-Pb Dating and Geochemical Characteristics. *Acta Petrologica Sinica*, 27(7): 2184–2194 (in Chinese with English Abstract)

Zhai, X. X., Yun, L., 2008. Geology of Giant Tahe Oilfield and a Review of Exploration Thinking in the Tarim Basin. *Oil and Gas Geology*, 9(5): 565–574 (in Chinese with English Abstract)

Zhao, W. Z., Zou, C. N., Feng, Z. Q., et al., 2008. Geological Features and Evaluation Techniques of Deep-Deated Volcanic Gas Reservoirs Songliao Basin. *Petroleum Exploration and Development*, 35(2): 129–142 (in Chinese with English Abstract)